ISSN: 0067-2904

Effect of Rotation on Peristaltic Flow of Sutterby Fluid through a Wave Channel

Fatima Khalid moean*, Dheia G. Salih Al-Khafajy
Department of Mathematics, College of Science, University of Al-Qadisiyah, Diwaniya, Iraq.

Received: 19/11/2023 Accepted: 18/8/2024 Published: 30/8/2025

Abstract

This study intends to investigate the effect of rotation on the peristaltic transport of non-Newtonian Sutterby fluid through wave channel. The equations are non-homogeneous and non-linear partial differential equations. The equations have been resolved using approximation long wavelength assumptions. The results have been examined through graphics using the "Mathematica 13" program. Therefore, it has been noticed that the effect of the flow rate, amplitude ratio, density of the fluid, viscosity of the fluid, rotation and tube's average radius on the distribution of velocity, pressure gradient, pressure rise, friction forces and stream function. It has been noticed by increasing the flow rate, amplitude ratio, density of the fluid and Sutterby fluid parameter, the velocity of fluid increases, but the fluid's velocity decreases while the viscosity of the fluid increases.

Keywords: Peristaltic flow, Sutterby Fluid, Wave Channel, Rotation, Cartesian coordinates.

تأثير الدوران على التدفق التمعجي لمائع سوتربي عبر قناة موجية

فاطمة خالد معين *, ضياء غازي صالح
قسم الرياضيات، كلية العلوم، الجامعة القادسية، القادسية، العراق.

الخلاصة

في هذا البحث تم دراسة تأثير الدوران على التدفق التمعجي لمائع سوتربي غير النيوتروني عبر القناة الموجية. المعادلات هي معادلات تفاضلية جزئية غير متجانسة غير خطية. تم حل المعادلات باستخدام افتراض تقريب طول الموجي الطويل. تم تحليل النتائج من خلال الرسوم البيانية باستخدام برنامج"13 "Mathematica، ولوحظ تأثير معدل الجريان ونسبة السعة وكثافة المائع ولزوجة المائع والدوران ومتوسط نصف قطر الأنبوب على توزيع السرعة وتدرج الضغط وارتفاع الضغط وقوى الاحتكاك. وقد لوحظ ان بزيادة معدل الجريان ونسبة السعة وكثافة المائع ومعلمة سائل سوتربي تزداد سرعة المائع، بينما تتناقص سرعة المائع بزيادة اللزوجة.

1. Introduction

Peristaltic motion is phenomena that happens when an extensible tube expands and contracts in a fluid, creating progressive waves that go down the length of the tube, mixing the fluid and moving it in the direction of the waves [1]. The contractions of the small

*Email: fatimakhalid19981116@gmail.com

intestine, known as peristalsis, play a crucial role in facilitating normal digestive processes. In addition to this, urine is transported from the kidney to the bladder via the ureter, Semen, on the other hand, moves through the vas deferens, lymphatic fluid is transported through lymphatic vessels, while bile flows from the gall bladder into the duodenum [2]. In research pertaining to mechanical and physiological processes, Latham [3] was the first proposed the concept of fluid transfer by peristaltic waves. The use of peristaltic motion has been extensively employed in many industrial and engineering applications. For instance, peristaltic motion may be effectively employed in the of wastewater slurries, sodium bromide, and slurry pumping. The utilisation of peristaltic motion in industrial fluid mechanics encompasses various applications involving aggressive chemicals, high solid slurries, noxious substances (such as those found in nuclear industries), and other materials that are transported using peristaltic pumps, roller pumps, hose pumps, tube pumps, heart-lung machines, blood pump machines, and dialysis machines, These engineering designs are based on the principle of peristalsis [2]. The phenomenon of rotation has extensive applications in cosmic and geophysical movements, contributing to a deeper understanding of galaxy formation and ocean circulation. Batool and Ahmed [4], Examined the Ree-Eyring liquid's peristaltic movement in a rotating frame while taking the convective situation into consideration. In [5], examines the impact of rotation and magnetic force on the waveform flow of a non-Newtonian fluid through a porous medium in a non-symmetric sloping canal. There are types of fluids such as Newtonian fluids like water and air, and non-Newtonian fluids are quite frequent like toothpaste [6]. The majority of technological and practical applications for the modification of natural phenomena favour viscoelastic non-Newtonian fluid over Newtonian fluid. Sutterby fluid, which represents fundamental equations for highly aqueous polymer solutions is a very important non-Newtonian fluid [7]. Numerous academic investigations rely on the utilisation of non-Newtonian fluids. Khan et al. [8], analyzed the Sutterby fluid flow by a rotating disk with homogeneous-heterogeneous reactions. Neeran and Hayat [9], focused on the impact of the endoscope on the peristaltic flow of Sutterby fluid.

In our study, we provide a mathematical model to examine the impact of rotation on the peristaltic transport of Sutterby fluid through wave channel. To solve the problem, we used the perturbation technique. The effect of parameters is analyzed and discussed through graphs of velocity, pressure gradient, pressure rise, friction forces, and stream functions.

2. Mathematical Formulation

Let us consider the peristaltic flow of Sutterby fluid through a regular channel, where the equation of the flow channel wall is in the form of a sine wave $\mp\left(d-\bar{\emptyset}\,sin^2\left(\frac{\pi}{\omega}(\bar{X}-s\bar{t})\right)\right)$ in Cartesian coordinates, where the positive sign represents the upper wall while the negative sign represents the lower wall of the channel. And d is the average radius of the tube, $\bar{\emptyset}$ is the amplitude of a peristaltic wave, ω is a wavelength, s is a wave propagation speed, and $\bar{t}$ is a time.

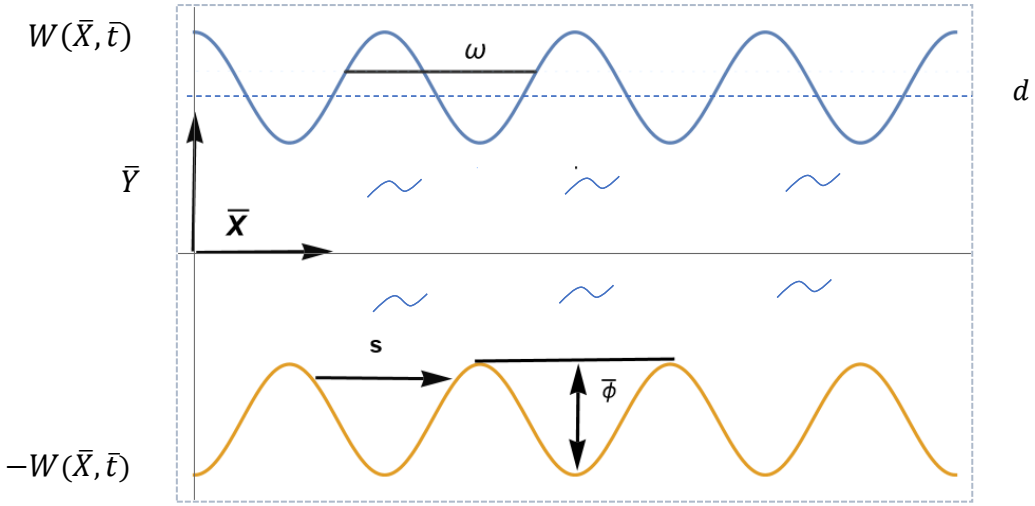

Figure 1: The geometry of problem.

The basic governing equations of the system are the continuity and Navier-Stokes equations with a rotation frame, given by:

$$\nabla.\bar{U} = 0. \quad \text{(continuity equation)} \tag{1}$$

$$\rho(\bar{U}.\nabla)\bar{U} + \rho\Omega\left((\Omega \times \bar{U}) + 2\frac{\partial \bar{U}}{\partial \bar{t}}\right) = \nabla\bar{S}. \quad \text{(momentum equation)} \tag{2}$$

The definition of Sutterby fluid equations is, [7, 9]:

$$\bar{S} = -\bar{p}I + \bar{\tau}. \tag{3}$$

$$\bar{\tau} = \frac{\mu}{2}\left[\frac{sinh^{-1}(b\dot{\gamma})}{b\dot{\gamma}}\right]^n (\nabla\bar{U} + (\nabla\bar{U})^T). \tag{4}$$

Here $\bar{U}$ is velocity filed, Ω is the rotation parameter, $\bar{p}$ is the pressure, I is the unit tensor, $\bar{\tau}$ is the extra stress tensor, μ_0 is the zero shear rate viscosity, and $\dot{\gamma}$ is the second invariant strain tensor which is defined as $\dot{\gamma} = \frac{1}{\sqrt{2}}\sqrt{trac(\nabla\bar{U} + (\nabla\bar{U})^T)^2}$, where $(\nabla\bar{U})$ is a gradient of the fluid velocity, and $(\nabla\bar{U})^T$ is the transpose of the gradient velocity in the Cartesian coordinates system (x, y, z). When $|b\dot{\gamma}| \ll 1$, we have $sinh^{-1}(b\dot{\gamma}) \approx (b\dot{\gamma}) - \frac{(b\dot{\gamma})^3}{6}$, so that equation (4) become:

$$\bar{\tau} \approx \frac{\mu}{2}\left[1 - \frac{nb^2}{6}(\dot{\gamma})^2\right](\nabla\bar{U} + (\nabla\bar{U})^T). \tag{5}$$

3. Solution of problem

Let $\bar{U}_1$ and $\bar{U}_2$ be the respective velocity components in the radial and axial directions in the fixed frame, respectively. The equations (1), (2), and (5) may be written as follows:

$$\frac{\partial \bar{U}_1}{\partial \bar{X}} + \frac{\partial \bar{U}_2}{\partial \bar{Y}} = 0. \tag{6}$$

$$\rho\left(\frac{\partial \bar{U}_1}{\partial \bar{t}} + \bar{U}_1\frac{\partial \bar{U}_1}{\partial \bar{X}} + \bar{U}_2\frac{\partial \bar{U}_1}{\partial \bar{Y}}\right) - \rho\Omega\left(\Omega\bar{U}_1 + 2\frac{\partial \bar{U}_1}{\partial \bar{t}}\right) = -\frac{\partial \bar{P}}{\partial \bar{X}} + \frac{\partial \bar{\tau}_{\bar{X}\bar{X}}}{\partial \bar{X}} + \frac{\partial \bar{\tau}_{\bar{X}\bar{Y}}}{\partial \bar{Y}}. \tag{7}$$

$$\rho\left(\frac{\partial \bar{U}_2}{\partial \bar{t}} + \bar{U}_1\frac{\partial \bar{U}_2}{\partial \bar{X}} + \bar{U}_2\frac{\partial \bar{U}_2}{\partial \bar{Y}}\right) - \rho\Omega\left(\Omega\bar{U}_2 - 2\frac{\partial \bar{U}_1}{\partial \bar{t}}\right) = -\frac{\partial \bar{P}}{\partial \bar{Y}} + \frac{\partial \bar{\tau}_{\bar{Y}\bar{X}}}{\partial \bar{X}} + \frac{\partial \bar{\tau}_{\bar{Y}\bar{Y}}}{\partial \bar{Y}}. \tag{8}$$

And the components of extra stress are, [7, 9]:

$$\bar{\tau}_{\bar{X}\bar{X}} = \frac{\mu}{2}\left[1 - \frac{nb^2}{6}\left\{2\left(\frac{\partial \bar{U}_1}{\partial \bar{X}}\right)^2 + 2\left(\frac{\partial \bar{U}_2}{\partial \bar{Y}}\right)^2 + \left(\frac{\partial \bar{U}_1}{\partial \bar{Y}} + \frac{\partial \bar{U}_2}{\partial \bar{X}}\right)^2\right\}\right]\left(2\frac{\partial \bar{U}_1}{\partial \bar{X}}\right).$$

$$\bar{\tau}_{\bar{X}\bar{Y}} = \frac{\mu}{2}\left[1 - \frac{nb^2}{6}\left\{2\left(\frac{\partial \bar{U}_1}{\partial \bar{X}}\right)^2 + 2\left(\frac{\partial \bar{U}_2}{\partial \bar{Y}}\right)^2 + \left(\frac{\partial \bar{U}_1}{\partial \bar{Y}} + \frac{\partial \bar{U}_2}{\partial \bar{X}}\right)^2\right\}\right]\left(\frac{\partial \bar{U}_1}{\partial \bar{Y}} + \frac{\partial \bar{U}_2}{\partial \bar{X}}\right).$$

$$\bar{\tau}_{\bar{Y}\bar{Y}} = \frac{\mu}{2}\left[1 - \frac{nb^2}{6}\left\{2\left(\frac{\partial \bar{U}_1}{\partial \bar{X}}\right)^2 + 2\left(\frac{\partial \bar{U}_2}{\partial \bar{Y}}\right)^2 + \left(\frac{\partial \bar{U}_1}{\partial \bar{Y}} + \frac{\partial \bar{U}_2}{\partial \bar{X}}\right)^2\right\}\right]\left(2\frac{\partial \bar{U}_2}{\partial \bar{Y}}\right).$$

By converting constant formulas from the test frame $(\bar{X}, \bar{Y})$ to the wave frame $(\bar{x}, \bar{y})$ with the relations:

$$\bar{u}_1(\bar{x}, \bar{y}) = \bar{U}_1(\bar{X} - s\bar{t}, \bar{Y}, \bar{t}) - s, \bar{u}_2(\bar{x}, \bar{y}) = \bar{U}_2(\bar{X} - s\bar{t}, \bar{Y}, \bar{t}), \bar{p}\,(\bar{x}, \bar{y}) = \bar{P}\,(\bar{X} - s\bar{t}, \bar{Y}, \bar{t}), \quad (9)$$

where $(\bar{u}_1, \bar{u}_2)$ and $(\bar{U}_1, \bar{U}_2)$ are velocity components of the moving and stationary structures. In order to simplify the governing equations of the problem, we might introduce the following dimensionless transformations as follow:

$$\left.\begin{aligned} x = \frac{\bar{x}}{\omega}, y = \frac{\bar{y}}{d}, u_1 = \frac{\bar{u}_1}{s}, u_2 = \frac{\omega \bar{u}_2}{sd}, p = \frac{d^2\bar{p}}{\mu\omega s}, \Psi = \frac{\bar{\Psi}}{ds}, R_e = \frac{\rho s d}{\mu}, \\ Q_1 = \frac{\bar{Q}_1}{ds}, q_1 = \frac{\bar{q}_1}{ds}, w = \frac{\bar{w}}{d}, \epsilon = \frac{nb^2s^2}{2d^2}, \delta = \frac{d}{\omega}, \emptyset = \frac{\bar{\emptyset}}{d}, \\ , \tau_{xx} = \frac{\omega\,\bar{\tau}_{\bar{x}\bar{x}}}{\mu s}, \tau_{xy} = \frac{d\bar{\tau}_{\bar{x}\bar{y}}}{\mu s}, \tau_{yy} = \frac{\omega\,\bar{\tau}_{\bar{y}\bar{y}}}{\mu s}, \end{aligned}\right\} \quad (10)$$

where R_e is the Reynolds number, $\emptyset$ is the amplitude ratio, δ is the dimensionless wave number, Ψ is the stream function, q_1 is the rate of flow and ϵ is the Sutterby fluid parameter. Substituting the non-dimensional parameters from equations (10) into the equations (6) - (8) we have:

$$\frac{s}{\omega}\left(\frac{\partial u_1}{\partial x} + \frac{\partial u_2}{\partial y}\right) = 0. \quad (11)$$

$$R_e\delta\left((u_1 + 1)\frac{\partial u_1}{\partial x} + u_2\frac{\partial u_1}{\partial y}\right) - \frac{\rho d^2}{\mu}\Omega^2(u_1 + 1) = -\frac{\partial p}{\partial x} + \delta^2\frac{\partial \tau_{xx}}{\partial x} + \frac{\partial \tau_{xy}}{\partial y}. \quad (12)$$

$$R_e\delta^3\left((u_1 + 1)\frac{\partial u_2}{\partial x} + u_2\frac{\partial u_2}{\partial y}\right) - \delta^2\frac{\rho d^2}{\mu}\Omega^2 u_1 = -\frac{\partial p}{\partial y} + \delta^2\frac{\partial \tau_{yx}}{\partial x} + \delta^2\frac{\partial \tau_{yy}}{\partial y}. \quad (13)$$

The associated dimensionless boundary conditions:

$$u_1 = -1 \quad \text{at} \quad y = \pm w = \pm\left(1 - \emptyset sin^2(\pi x)\right). \quad (14)$$

The general solution of the governing equations (11)-(13) in the general case seems to be impossible, therefore, we shall confine the analysis under the assumption of small dimensionless wave number. It is followed that $\delta \ll 1$. So that the equations (11)-(13) become as:

$$\frac{\partial u_1}{\partial x} + \frac{\partial u_2}{\partial y} = 0. \quad (15)$$

$$-\frac{\rho d^2}{\mu}\Omega^2(u_1 + 1) = -\frac{\partial p}{\partial x} + \frac{\partial \tau_{xy}}{\partial y}. \quad (16)$$

$$-\frac{\partial p}{\partial y} = 0\,. \quad (17)$$

And the component of extra stress tensor become as the form:

$$\tau_{xy} = \left[\frac{\partial u_1}{\partial y} - \epsilon\left(\frac{\partial u_1}{\partial y}\right)^3\right]. \quad (18)$$

By substituting equation (18) into equation (16), we get:

$$-\frac{\rho d^2}{\mu}\Omega^2(u_1 + 1) = -\frac{\partial p}{\partial x} + \frac{\partial^2 u_1}{\partial y^2} - 3\epsilon\left(\frac{\partial u_1}{\partial y}\right)^2\frac{\partial^2 u_1}{\partial y^2}\,. \quad (19)$$

4. Rate of volume flow

The instantaneous volume flow rate in fixed coordinates system given by:

$$\hat{Q} = \int_{-W}^{W}\bar{U}_1(\bar{X} - s\bar{t}, \bar{Y},\ \bar{t})d\bar{Y}. \quad (20)$$

Using the transformation $(\bar{u}_1(\bar{x}, \bar{y}) + s)$ into equation (20) and then integrating it, we get:

$$\hat{Q} = \bar{q} + s(W + W) = \bar{q} + 2sW. \quad (21)$$

Where $\bar{q} = \int_{-W}^{W} \bar{u}_1(\bar{x}, \bar{y}) d\bar{y}$. From equations (10), we have $q = \int_{-W}^{W} u_1 \, dy$.
The time means flow rate over a period $T = \frac{\omega}{s}$ at a fixed position is definede as:

$$\bar{Q} = \frac{1}{T}\int_0^T \hat{Q} \; d\bar{t}. \tag{22}$$

Substituting equation (21) in equation (22), we will obtain:

$$\bar{Q} = \frac{1}{T}\int_0^T (\bar{q} + 2sW)\, d\bar{t} = \bar{q} + 2s\left(d - \frac{\bar{\emptyset}}{2}\right). \tag{23}$$

By using dimensionless transformations in equation (10) into the equation (23), we have
$dsQ = dsq + 2s\left(d - \frac{d\emptyset}{2}\right)$, hence, we get

$$q = Q + \emptyset - 2. \tag{24}$$

5. Method of solution

The equation (17) shows that p dependents only on x. Equation (19) becomes as:

$$\frac{\partial^2 u_1}{\partial y^2} + A u_1 = \frac{dp}{dx} - A + 3\epsilon \left(\frac{\partial u_1}{\partial y}\right)^2 \frac{\partial^2 u_1}{\partial y^2}. \tag{25}$$

Where $A = \frac{\rho d^2}{\mu}\Omega^2$.
Equation (25) is a non-linear differential equation and it is difficult to find an exact solution, so we will use the perturbation technique to find the problem solution, as follows:

$$u_1 = u_{10} + \epsilon\, u_{11} + O(\epsilon^2). \tag{26}$$
$$p = p_0 + \epsilon\, p_1 + O(\epsilon^2). \tag{27}$$
$$\Psi = \Psi_0 + \epsilon\, \Psi_1 + O(\epsilon^2). \tag{28}$$
$$q = q_0 + \epsilon\, q_1 + O(\epsilon^2). \tag{29}$$

Substituting equations (26) and (27) into equation (25), then, by equating the similar powers of ϵ, we get the following results presented in the following subsections:

i – Zero-o system (ϵ^0)

$$\frac{\partial^2 u_{10}}{\partial y^2} + A u_{10} = \frac{dp_0}{dx} - A. \tag{30}$$

The associated boundary conditions $u_{10} = -1$ at $y = \pm w = \pm\left(1 - \emptyset sin^2(\pi x)\right)$.
And $q_0 = \int_{-W}^{W} u_{10} dy$ where $q_0 = Q_0 + \emptyset - 2$. (31)

***ii* – First-Order System (ϵ^1)**

$$\frac{\partial^2 u_{11}}{\partial y^2} + A u_{11} = \frac{dp_1}{dx} + 3\left(\frac{\partial u_{10}}{\partial y}\right)^2 \frac{\partial^2 u_{10}}{\partial y^2}. \tag{32}$$

The associated boundary conditions $u_{11} = 0$ at $y = \pm w = \pm(1 - \emptyset sin^2(\pi x))$.
And $q_1 = \int_{-w}^{w} u_{11}\, dy$ where $q_1 = Q_1$. (33)
From the solution of the equations (30) and (32), and substitution the resulting in (26), we get:

$$u_1 = \left(-\frac{Sec[\sqrt{A}w]\left(\frac{dp_0}{dx}\right)}{A}\right) Cos\left[\sqrt{A}y\right] + \frac{-A + \left(\frac{dp_0}{dx}\right)}{A} +$$

$$\epsilon\left(\left(-\frac{1}{32A^2} Sec\left[\sqrt{A}w\right]^3 \left(12Cos\left[2\sqrt{A}w\right]\left(\frac{dp_0}{dx}\right)^3 - 3Cos\left[4\sqrt{A}w\right]\left(\frac{dp_0}{dx}\right)^3 + \right.\right.\right.$$

$$32ACos\left[\sqrt{A}w\right]^4 \left(\frac{dp_1}{dx}\right) + 32ACos\left[\sqrt{A}w\right]^2 Sin\left[\sqrt{A}w\right]^2 \left(\frac{dp_1}{dx}\right) + 12\sqrt{A}w\left(\frac{dp_0}{dx}\right)^3 Tan\left[\sqrt{A}w\right] -$$

$$\left.\left.\left. 3Sin\left[4\sqrt{A}w\right]\left(\frac{dp_0}{dx}\right)^3 Tan\left[\sqrt{A}w\right]\right)\right) Cos\left[\sqrt{A}y\right] +$$

$$\frac{1}{32A^2}\Big(12Cos[\sqrt{A}y]Cos[2\sqrt{A}y]Sec[\sqrt{A}w]^3\left(\frac{dp_0}{dx}\right)^3 - 3Cos[\sqrt{A}y]Cos[4\sqrt{A}y]Sec[\sqrt{A}w]^3\left(\frac{dp_0}{dx}\right)^3 + 12\sqrt{A}ySec[\sqrt{A}w]^3Sin[\sqrt{A}y]\left(\frac{dp_0}{dx}\right)^3 - 3Sec[\sqrt{A}w]^3Sin[\sqrt{A}y]Sin[4\sqrt{A}y]\left(\frac{dp_0}{dx}\right)^3 + 32ACos[\sqrt{A}y]^2\left(\frac{dp_1}{dx}\right) + 32ASin[\sqrt{A}y]^2\left(\frac{dp_1}{dx}\right)\Big)\Big). \quad (34)$$

6. Pressure rise, friction forces, and stream function

The expression for the pressure rises Δp_Ω and friction forces on the upper and lower walls F_Ω is defined as follows:

$$\Delta p_\Omega = \int_0^1 \left(\frac{dp}{dx}\right) dx. \quad (35)$$

$$F_\Omega = \int_0^1 w^2 \left(-\frac{dp}{dx}\right) dx. \quad (36)$$

The corresponding stream function is $\Psi = \Psi_0 + \epsilon\Psi_1 = \int u_{10}\, dy + \epsilon \int u_{11}\, dy$.

7. Numerical results and discussion

In this section, we discuss graphically, and by using Mathematica 13 programme, the effect of the rotation and some other factors on peristaltic flow, pressure gradient, frictional forces, and the stream function of a Sutterby fluid through a wave channel.

7.1 Velocity distribution

We analysed and discussed through Figures (2-4) the effect of parameters $\rho, \mu, Q_0 = Q_1, \emptyset, d$ and ϵ on fluid velocity. Figure (2) shows that the velocity u_1 increases when the density of fluid ρ increases at the middle of the channel, while the velocity u_1 decreases when fluid's viscosity μ increases at the middle of the channel, but the velocity u_1 increases when the viscosity μ increases near the channel's walls. In Figure (3) we notice velocity u_1 increases when $Q_0 = Q_1$ and $\emptyset$ increases. Figure (4) shows the velocity u_1 increases at the middle of the channel when d increases, but decreases near the channel's walls, while its increasing when ϵ increases.

7.2 Pressure gradient

The Figures (5-7) show the effect of parameters $Q_0 = Q_1, \epsilon, \emptyset, \rho, \Omega$ and μ on pressure gradient dp/dx. Figures (5) and (6) show that the pressure gradient decreases when $Q_0 = Q_1, \epsilon, \emptyset$ and ρ increasing. In Figure (7) we notice the pressure gradient decreases with increases Ω, but its increasing when μ increases.

Figures (8-10) illustrate the effects of the parameters $Q_0 = Q_1, \epsilon, \emptyset, \rho, d$ and μ for the pressure rise ΔP_Ω at the region $1 < \Omega < 1.3$. Figures (8) and (9), show that ΔP_Ω increasing when $Q_0 = Q_1, \epsilon, \emptyset$ and ρ increases. We can see in Figure (10), ΔP_Ω increases with an increasing in parameter d, but it decreasing when μ increasing.

7.3 Friction force

Figures (11-13) show the effect of parameters $Q_0 = Q_1, \epsilon, \emptyset, \rho, d$ and μ on friction force distribution F_Ω. In Figures (11) and (12), we notice the friction force decreasing when $Q_0 = Q_1, \epsilon, \emptyset$ and ρ increases. Figure (13), show that the friction force decreases when d increasing, but its increases when μ increasing.

7.4 Phenomena trapping

A description the process by which closed stream function create an internally circulating bolus of fluid, which is then pushed forward by the propagating peristaltic wave is known as

trapping phenomenon. the results on trapping can be seen illustrated in Figures (14-20). In Figure (14), we notice by increasing the flow rate $Q_0 = Q_1$ the bolus size gradually increases. Figures (15) and (16), show that the bolus increases when $\emptyset$ and density of fluid increasing. In Figure (17), we notice that when the fluid's viscosity μ increases, leads to decreases in the bolus volume at the lower and upper walls of the channel gradually. Figures (18-20), show that by increasing d, Ω and ϵ the bolus size gradually increases at the lower and upper walls of the channel.

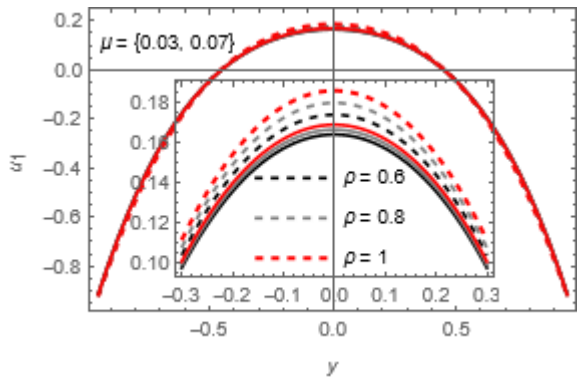

Figure 2: Velocity distribution for various values ρ and μ at $Q_0 = Q_1 = 1.2, \emptyset = 0.25, d = 0.8, \Omega = 0.2, \epsilon = 0.2, x = 0.1$

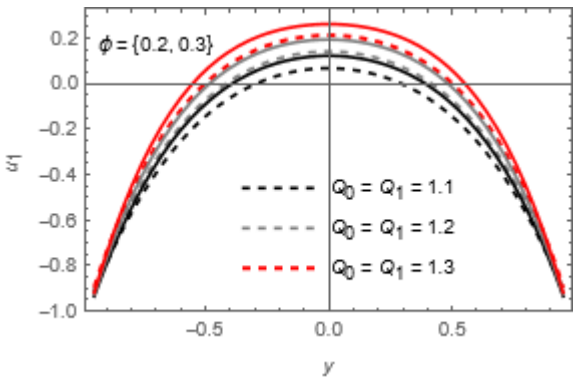

Figure 3: Velocity distribution for various values $Q_0 = Q_1$ and $\emptyset$ at $\rho = 0.8, \mu = 0.07, d = 0.8, \epsilon = 0.2, \Omega = 0.2, x = 0.1$

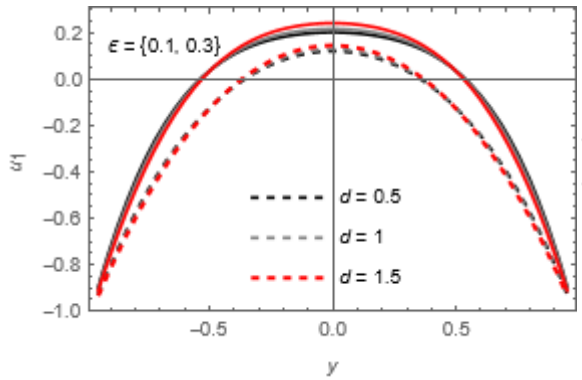

Figure 4: Velocity distribution for various values d and ϵ at $Q_0 = Q_1 = 1.2, \emptyset = 0.25, \rho = 0.8, \mu = 0.07, \Omega = 0.2, x = 0.1$

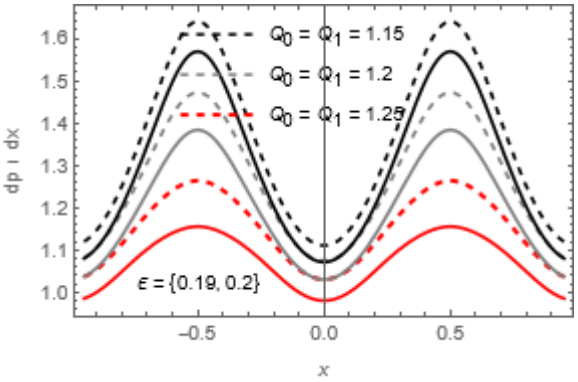

Figure 5: Pressure gradient for various values of $\emptyset = 0.25, \mu = 0.07, \Omega = 0.2, d = 0.8, \rho = 0.8$

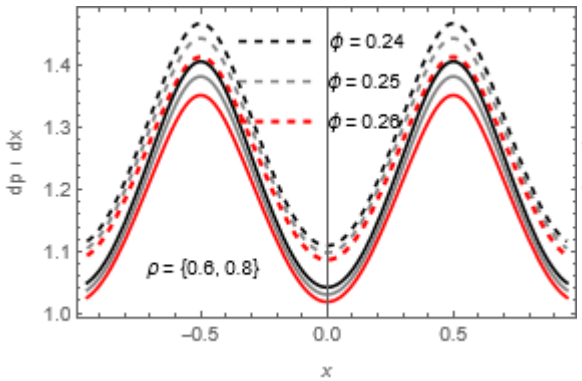

Figure 6: Pressure gradient for various values of $Q_0 = Q_1 = 1.2, \mu = 0.07, d = 0.8, \epsilon = 0.2, \Omega = 0.2$

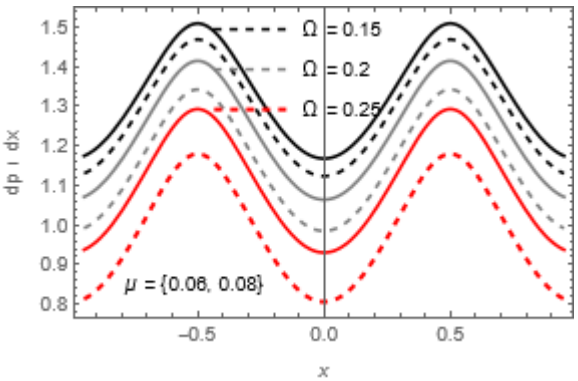

Figure 7: Pressure gradient for various values of $Q_0 = Q_1 = 1.2, \emptyset = 0.25, \rho = 0.8, d = 0.8, \epsilon = 0.2$

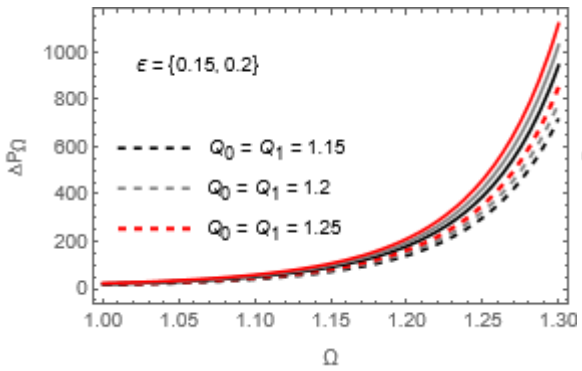

Figure 8: Pressure rise for various values of $\emptyset = 0.25, \rho = 0.8, d = 0.8, \mu = 0.07$

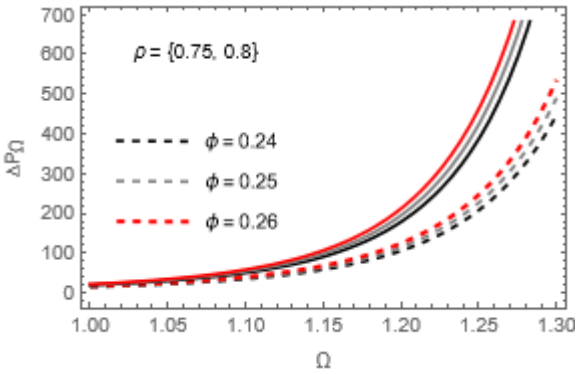

Figure 9: Pressure rise for various values of $Q_0 = Q_1 = 1.2, \mu = 0.07, d = 0.8, \epsilon = 0.2$

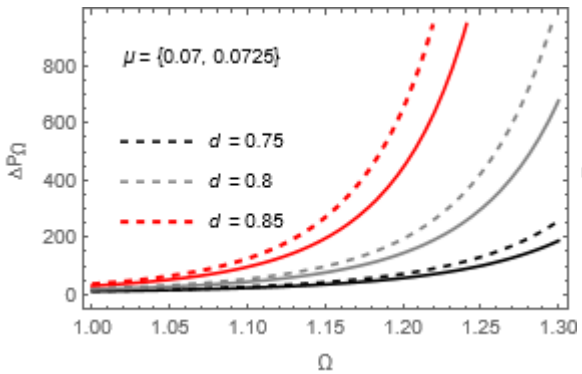

Figure 10: Pressure rise for various values of $Q_0 = Q_1 = 1.2, \emptyset = 0.25, \rho = 0.8, \epsilon = 0.2$

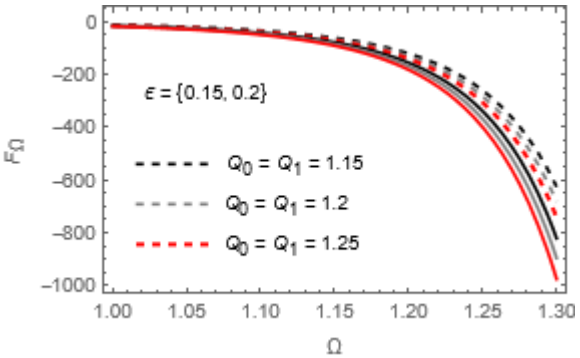

Figure 11: Frictions forces for various values of $\emptyset = 0.25, \rho = 0.8, d = 0.8, \mu = 0.07$

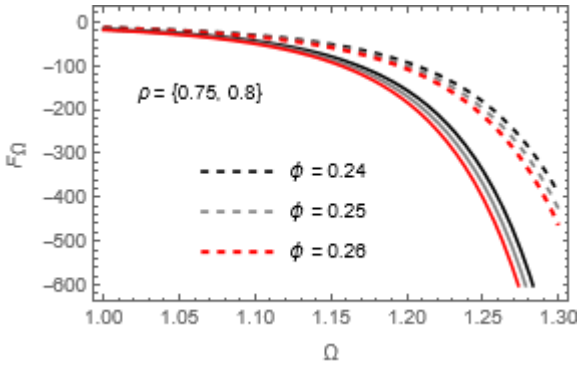

Figure 12: Frictions forces for various values of $Q_0 = Q_1 = 1.2, \mu = 0.07, d = 0.8, \epsilon = 0.2$

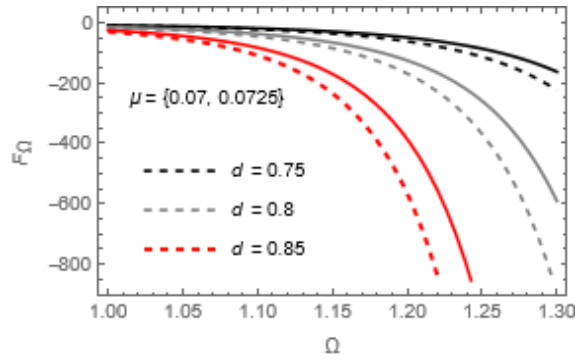

Figure 13: Frictions forces for various values of $Q_0 = Q_1 = 1.2, \emptyset = 0.25, \rho = 0.8, \epsilon = 0.2$

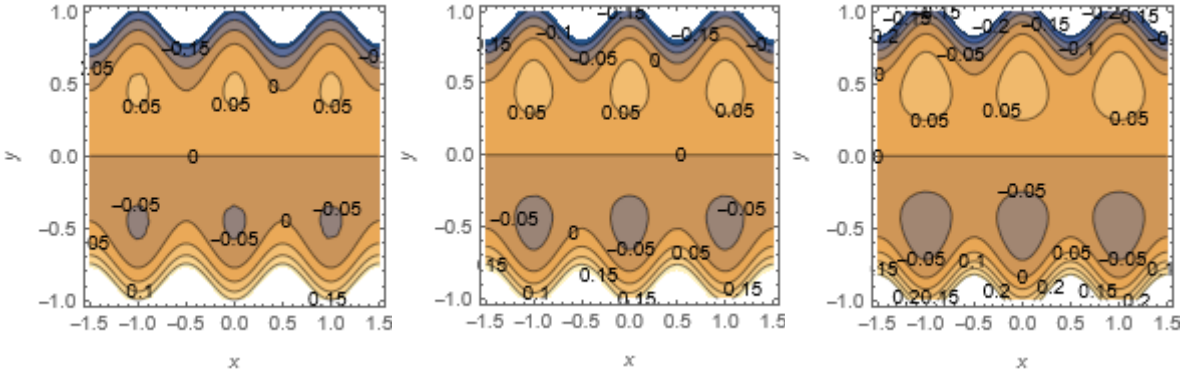

Figure 14: Stream function with various values of $Q_0 = Q_1 = \{1.2,1.23,1.26\}$ at $\emptyset = 0.25, \rho = 0.8, \mu = 0.07, \Omega = 0.2, d = 0.8, \epsilon = 0.2$

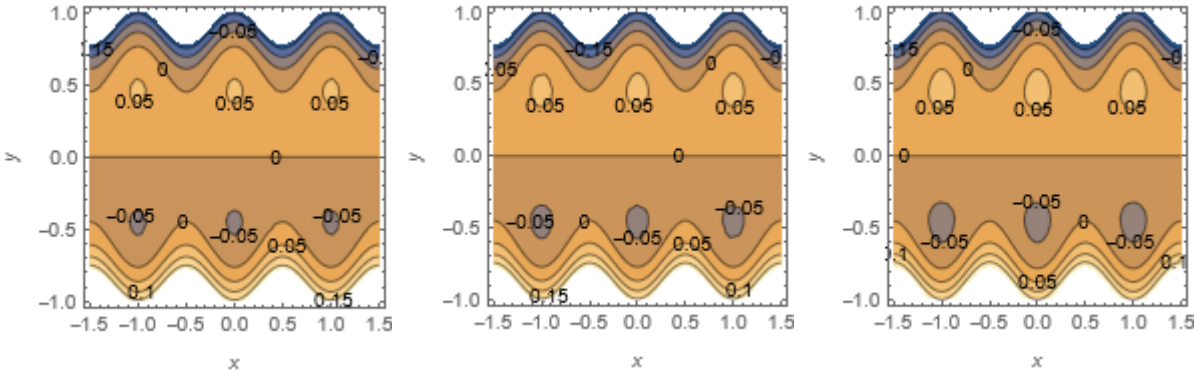

Figure 15: Stream function with various values of $\emptyset = \{0.24,0.25,0.26\}$ at $Q_0 = Q_1 = 1.2, \rho = 0.8, \mu = 0.07, \Omega = 0.2, d = 0.8, \epsilon = 0.2$

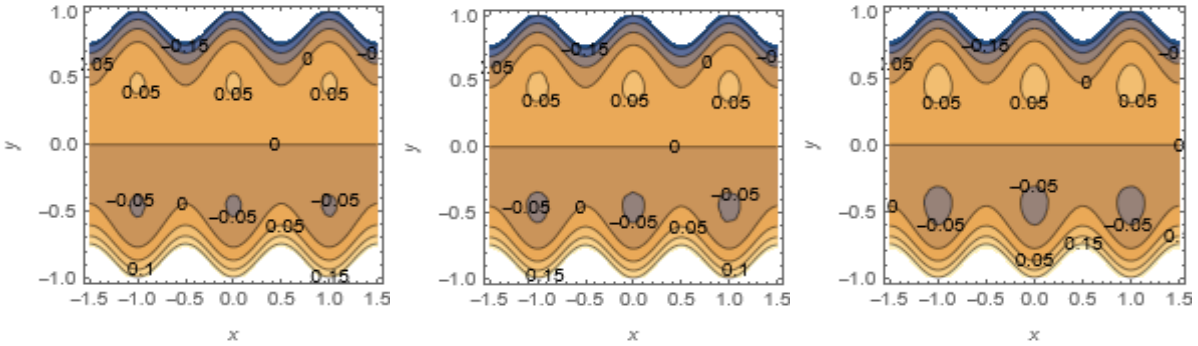

Figure 16: Stream function with various values of $\rho = \{0.1,0.8,1.6\}$ at $Q_0 = Q_1 = 1.2, \emptyset = 0.25, \mu = 0.07, \Omega = 0.2, d = 0.8, \epsilon = 0.2$

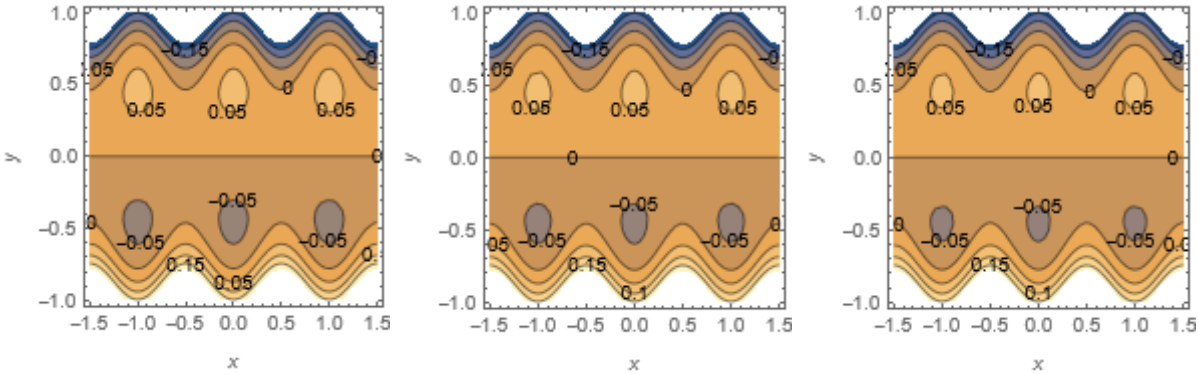

Figure 17: Stream function with various values of $\mu = \{0.03,0.04,0.06\}$ at $Q_0 = Q_1 = 1.2, \emptyset = 0.25, \rho = 0.8, \Omega = 0.2, d = 0.8, \epsilon = 0.2$

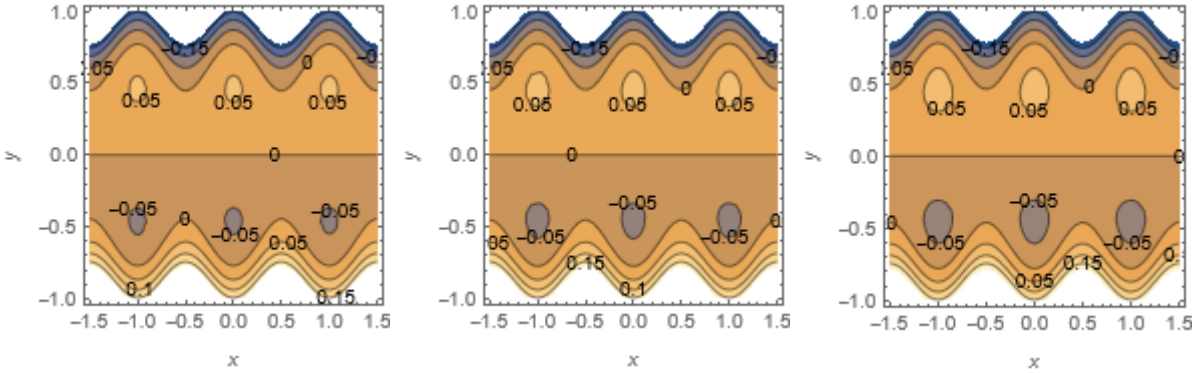

Figure 18: Stream function with various values of $d = \{0.5,0.9,1.2\}$ at $Q_0 = Q_1 = 1.2, \emptyset = 0.25, \rho = 0.8, \mu = 0.07, \Omega = 0.2, \epsilon = 0.2$

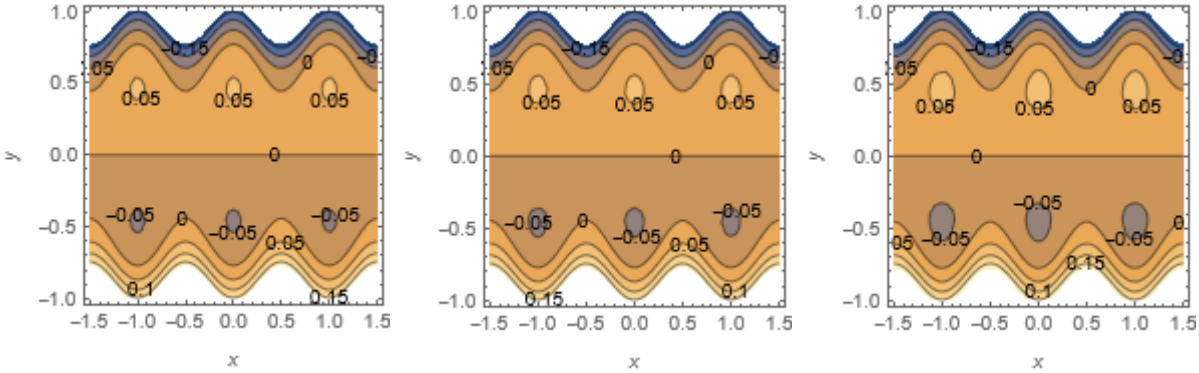

Figure 19: Stream function with various values of $\Omega = \{0.05,0.15,0.25\}$ at $Q_0 = Q_1 = 1.2, \emptyset = 0.25, \rho = 0.8, \mu = 0.07, d = 0.8, \epsilon = 0.2$

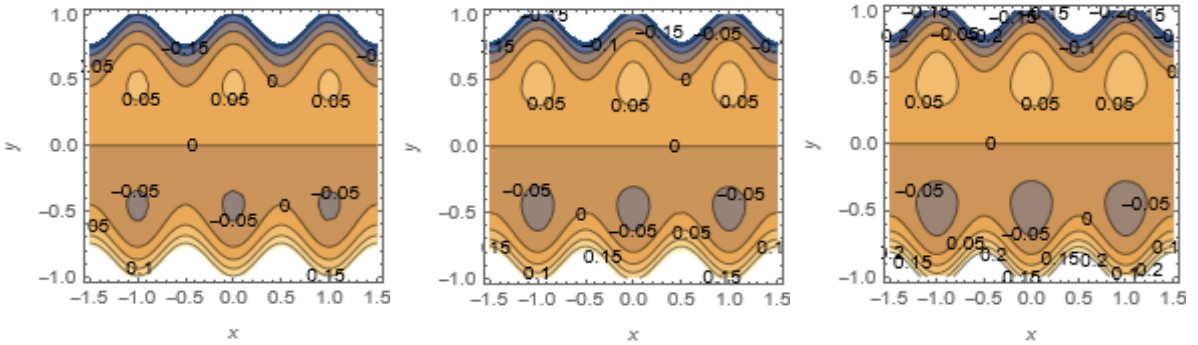

Figure 20: Stream function with various values of $\epsilon = \{0.2,0.225,0.25\}$ at $Q_0 = Q_1 = 1.2, \emptyset = 0.25, \rho = 0.8, \mu = 0.07, \Omega = 0.2, d = 0.8$

8. Conclusions

Here, we investigate the effects of rotation on peristaltic flow of Sutterby fluid through a wave channel. We used the Mathematica"13" program to discuss the effect of parameters on the movement of liquids by explaining the graphs obtained, and we found that by increasing the parameters $\rho, Q_0 = Q_1, \emptyset$ and ϵ leads to increases in fluid's velocity, and fluid's velocity increasing in the middle of the channel, with an increases in d, but its decreases near the walls of the channel, while with an increases in the viscosity μ leads to decreases in fluid's velocity. The pressure gradient dp/dx of fluid increases with increases in the parameter μ, while it decreases when $Q_0 = Q_1, \epsilon, \emptyset, \rho$ and Ω increasing. Pressure rise increasing under the effect of parameters $Q_0 = Q_1, \epsilon, \emptyset, \rho$ and d, but it decreases when the parameters μ increasing. Friction forces increases when the parameter μ increases, while its decreasing when the parameters $Q_0 = Q_1, \epsilon, \emptyset, \rho$ and d increases. The trapped bolus is expanding with

the increase in the parameters $Q_0 = Q_1, \emptyset, \rho, d, \Omega$ and ϵ, while the increases in the viscosity of fluid μ, leads to decreases in the bolus volume gradually.

References

[1] N. T. M. Eldabe, B. M. Agoor, and H. Alame, "Peristaltic motion of non-Newtonian fluid with heat and mass transfer through a porous medium in channel under uniform magnetic field," *Journal of Fluids,* 2014.

[2] H. N. Mohaisen, A. M. Abedulhadi, "Effects of the Rotation on the Mixed Convection Heat Transfer Analysis for the Peristaltic Transport of Viscoplastic Fluid in Asymmetric Channel," *Iraqi Journal of Science,* vol. 63, no. 3, pp. 1240-1257, 2022.

[3] T.W. Latham, Fluid Motion in a Peristaltic Pump, Massachusetts Institute of Technology, 1966.

[4] B. A. Almusawi, A. M. Abdulhadi, "Heat Transfer Analysis and Magnetohydrodynamics Effect on Peristaltic Transport of Ree–Eyring Fluid in Rotating Frame," *Iraqi Journal of Science,* vol. 62, no. 8, pp. 2714-2725, 2021.

[5] T. Sh. Alshareef, "Impress of rotation and an inclined MHD on waveform motion of the non-Newtonian fluid through porous canal," *Journal of Physics: Conference Series ,* 2020.

[6] R. W. Fox, A. T. McDonald, and P. J. Pritchard, Introduction in fluid mechanics, John Wiley & Sons, 2004.

[7] T. Hayat, et al. "Sutterby fluid flow subject to homogeneous–heterogeneous reactions and nonlinear radiationl," *Physica A: Statistical Mechanics and Applications,* vol. 544, 2020.

[8] M. I. Khan, S. Qayyum, T. Hayat, and A. Alsaedi, "Stratified flow of Sutterby fluid with homogeneous-heterogeneous reactions and Cattaneo-Christov heat flux," *International Journal Of Numerical Methods for Heat and Fluid Flow,* vol. 29, no. 8, pp. 2977-2992, 2019.

[9] N. Ammar, H. A. Ali, "Mathematical Modelling for Peristaltic Flow of Sutterby Fluid Through Tube under the Effect of Endoscope," *Iraqi Journal of Science,* vol. 64, no. 5, pp. 2368-2381, 2023.